Modeling of Thermal Processes Associated to an Electric Arc

Allagui Hatem, Ghodbane Fathi

Abstract—The primary objective of this paper is to study the thermal effects of the electric arc on the breaker apparatus contacts for forecasting and improving the contact durability. We will propose a model which takes account of the main influence factors on the erosion contacts. This phenomenon is very complicated because the amount of ejected metal is not necessarily constituted by the whole melted metal bath but this depends on the balance of forces on the contact surface. Consequently, to calculate the metal ejection coefficient, we propose a method which consists in comparing the experimental results with the calculated ones. The proposed model estimates the mass lost by vaporization, by droplets ejection and by the extraction mechanism of liquid or solid metal. In the one-dimensional geometry, to calculate of the contact heating, we used Green's function which expresses the point source and allows the transition to the surface source. However, for the two- dimensional model we used explicit and implicit numerical methods. The results are similar to those found by Wilson's experiments.

Keywords—Electric arc, thermal effect, erosion, contact, durability.

I. INTRODUCTION

THE physics of electrical discharges has known considerable progress that helped to better define the processes related to the phenomena in the vicinity of the electrodes and the energy transfer in the arc column. Thus, several applications of the thermal effects of the arc have been developed [1], including welding, arc furnaces, metal processing, thermal plasma generators, electrical discharge machining and especially the breaking apparatus where the existence of the arc during the breaking phase avoids adverse effects on the network. The increase of the durability of electrical apparatuses (contactors, circuit breakers...) concerns manufacturers who always try to improve the silver, tungsten cadmium and copper based contacts. At the research level it is necessary to establish and develop the engineering methods to define the contact erosion of the equipment submitted to the effect of the electric arc [2]-[4]. The knowledge of the current density and the dimensions of the cathode and anode spots, through which the whole current passes, allow to model the thermal phenomenon in an electrode submitted to an electric arc. The thermal model will take into account the changes in the metal state (solid-liquid and liquid-vapor). To solve the thermal problem of the penetration of the melting and the vaporization border of the metal in function we use numerical and analytical methods.

This paper is divided into 6 main sections. Section I gives details about the thermal effects of the arc and their applications. Section II explains the electrodes phenomena. In Section III we will present the thermal model of the arc and its interaction with the contact material. Section IV is a description of the erosion measurements. Section V shows the erosion calculation method proposed and we will finish by a conclusion.

II. THE PROBLEM OF CALCULATING OF THE THERMAL EFFECTS OF THE ELECTRIC ARC

The arc is a very important phenomenon whose motion is governed by two mechanisms: a movement due to forces acting on the column and a movement due to the electrodes phenomena (especially at the cathode): gradually as one approaches the metal electrodes, there is a significant constriction of current lines which is commonly called the cathodic and anodic spot. The cathodic spot is an electron emitter to the arc column, which is formed by separate emissive centers, very scattered in the case of a vacuum arc and much closer to each other in the presence of an atmosphere. From the electrical point of view, the cathode spot is characterized by a very abrupt voltage drop between the metal and the adjacent gas. This is observed even for infinite arc lengths and the value of this drop is constant regardless of the surrounding gas and the pressure of the medium. The anode is a single electron collector and the mechanisms are simple. The constriction of the current lines to the anode spot is smaller than in the vicinity of the cathode, and the current densities are lower. The experimental observations show that the spot is more often single, circular and its size is comparable to the section of the plasma column. The arc column is plasma in which there are all types of particles, electrons, ions, but also atoms and molecules whose energies are equalized as a result of a local thermodynamic equilibrium. A qualitative aspect of the column assembly and arc electrodes is shown in Fig. 1.

Hatem Allagui is with Research Unit Analysis and Control Systems, ENIT, Campus Universitaire, El Manar, tunis, Tunisia (e-mail: hatem.allegui@enit.rnu.tn).
Ghodbane Fathi is with Electrical Systems Laboratory, ENIT, Campus Universitaire El Manar, Tunis, Tunisia (e-mail: ghodbanefathi@yahoo.fr).

World Academy of Science, Engineering and Technology
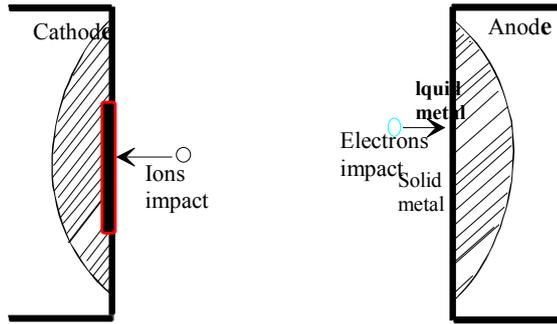International Journal of Electrical and Computer Engineering
Vol:7, No:11, 2013

Fig. 1 The electrodes phenomena

The thermal effects of the arc are dominated by two mechanisms: the first is the bombing of the structure on its surface by electrons and ions in the plasma zone near the electrodes. The second is a Joule effect due to the current flow (space charge). Since the heat flux density caused by the arc is high the surface temperature of the material increases up to melting and vaporization of the metal under the effect of the thermal energy supplied by the arc. [5] The development of a thermal model to calculate the dimensions of the melt and crater vaporization requires prior knowledge of the values of the heat flux.

III. THE THERMAL MODEL OF THE ELECTRIC ARC

The study of the arc interaction with the contact material takes us to the model heating of a plate at its center by an arc foot that provides a thermal flux Q whose density is equal to q (Fig. 2). The calculation is done during the stabilization (stagnation) of the arc.
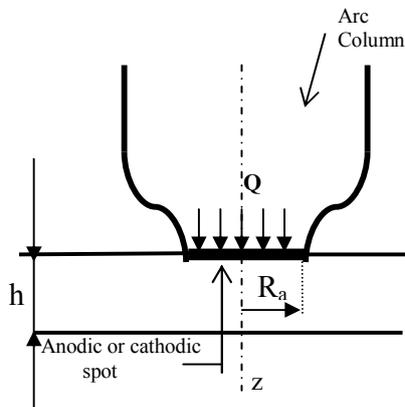

Fig. 2 Thermal model of the electric arc (Q: heat flux brought by the arc; R_a: radius of the cathodic or anodic spot; h: plate thickness)

In order to simplify the model, the power on the electrode surface is assumed to be uniform and the constant heat flux density ($q = q_0$).

A. The Mathematical Formulation

The metal electrode heats up under the surface effect of the heat flow brought by the arc. Assuming that the plate is thermally insulated ($Qi = 0$) and applying the heat equation:

$$\rho c \frac{\partial T}{\partial t} = \sigma\, div\left[\nabla T\right] + Qi \tag{1}$$

T is the temperature at any point of the plate;
t: time (s).
ρ: volume density of the material (kg/m^3)
σ: thermal conductivity (W/m °K)
c: specific heat (J/kg. ° K).
Qi: heat generated by internal sources (W/m^3).
Qi is the source term in the volume for example Joule effect which is caused by the passage of the current in the electrode through its surface. We have neglected this source relative to the surface source (Qi = 0).

Equation (1) becomes:

$$\frac{\partial T}{\partial t} = a\ div\ \left[\nabla T\right] \tag{2}$$

where **a** is called thermal diffusivity of the material, it is given by the following relationship:

$$a = \sigma/\rho c \ (m^2/s) \tag{3}$$

Add to (2) the boundary conditions (4), (5) and (6):

$$-\sigma \left.\frac{\partial T}{\partial z}\right|_{z=0} = q_0 \qquad r \leq Ra; \tag{4}$$

$$-\sigma \left.\frac{\partial T}{\partial z}\right|_{z=h} = 0 \qquad r \geq Ra; \tag{5}$$

$$T(r,z,0) = T_0 \tag{6}$$

where $\frac{\partial T}{\partial t}$ is the temperature variation along the z axis.

Since the thermal constant of a metal varies depending on the temperature, the thermal problem to be solved is considered non-linear. However, if the variation of c and ρ is low enough, they can be considered constant, if the variations of σ in each phase (solid and liquid) are very low, there will be a solid conductivity and liquid conductivity [6], the system becomes linear and (2) must be solved in each phase solid and liquid. In addition, since we have a change of phase (solid-liquid and liquid-vapor), we should also take the transition conditions between two media known as Stefan equations [7].

At the solid-liquid border:

$$\sigma_{liquide} \left.\frac{\partial T}{\partial n}\right|_{n=nfusion} + \sigma_{solide} \left.\frac{\partial T}{\partial n}\right|_{n=nfusion} = \rho\, Q_f\, V_f \tag{7}$$

At the liquid-vapor border:

$$q_0 + \sigma_{liquide} \left.\frac{\partial T}{\partial n}\right|_{n=nvap} \quad \rho\, Q_{vap}\, V_{vap} \tag{8}$$

World Academy of Science, Engineering and Technology
International Journal of Electrical and Computer Engineering
Vol:7, No:11, 2013

where:

V_f and V_{vap} are respectively the fusion speed and vaporization speed of the metal (m^3/s);

Q_f and are respectively the latent heat of fusion and vaporization.

For this resolution system, we used the numerical and analytical methods.

B. The Analytical Resolution Using the Source Method

Some authors [8] used conventional methods (functions tabulated calculation of integrals) proposing approximate formulas describing the penetration of the temperature in depth of the electrode by converting a two-dimensional problem into a one-dimensional one. The calculation is valid only if the size of the heat source is very small compared to the surface of the electrodes. However, it is interesting to look for solutions to the equation of heat conduction using the source method. In our case, the heat source is the foot of the arc, up to a very small radius from the surface of the electrode, and the thermal characteristics of the contact material are constant per phase (solid phase and liquid phase). The source method is widely used for solving thermal problems; it is expressed by Green's function. For the purpose of simplification, we transformed (2) into a system using cylindrical coordinates. In this system the position of each point of the electrode is determined by the polar coordinates (r, θ) and by the depth z (Fig. 3).
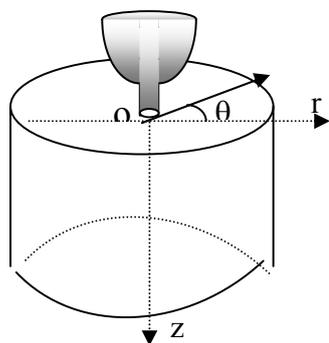

Fig. 3 Thermal model of the electric arc in cylindrical coordinates

The solution corresponding to (2), (4) and (5) for an instantaneous point heat source unit is of the type [8]:

$$G = \frac{\exp\left(\frac{-R^2}{4at}\right)}{8(\pi at)^{\frac{3}{2}}} \sum_{n=-\infty}^{n=+\infty} \left(\exp\left(\frac{-(2nh+z'-z)^2}{4at}\right) + \exp\left(\frac{-(2nh-z'-z)^2}{4at}\right)\right) \quad (9)$$

where:

G is the Green's function. In this case, G is taken as the temperature at a point M (x, y, z) at time t due to heating by an instantaneous source point installed at point M '(x', y ', z ') at time, t = 0.

$$R^2 = (x-x')^2 + (y-y')^2 = r^2 + r'^2 - 2rr'\cos(\theta-\theta') $$

(r,θ) and (r',θ') are respectively the polar coordinates of the points (x,y) and(x',y').

In the case of an action arc on the side walls of a plate having a relatively thin plate such as welding, plate, the wall plane, the storage reservoirs of flammable materials, it becomes interesting to consider the electrode as a thin plate. In this case study the Green's function is given by [8]:

$$G' = \frac{Q'}{4\pi\sigma h(t-t')} \exp\left(-\frac{r^2 + r'^2 - 2rr'\cos(\theta-\theta')}{4a(t-t')}\right) \quad (10)$$

G ' is in fact the temperature to a point M (x, y, z) at time t due to heating by an instantaneous source point generated at the point M'(x ', y', z ') to time t '.

Q' is the amount of heat generated at time t 'and the origin of coordinates:

$$Q' = q_0\, 2\pi\, r'\, dr'\, d\theta'\, dt' \quad (11)$$

The temperature at any point of the electrode is obtained by:

$$T(r,z,t) = \int_0^t \int_0^{R_a} \int_0^{2\pi} G'\, d\theta'\, dr'\, dt' \quad (12)$$

so:

$$T(r,t) = \int_0^t \int_0^{R_a} \int_0^{2\pi} \frac{q\,2\pi\,r'}{4\pi\sigma h(t-t')} \exp(F1)\, d\theta'\, dr'\, dt'$$

$$\text{avec } F1 = \left[-\frac{r^2 + r'^2 - 2rr'\cos(\theta-\theta')}{4a(t-t')}\right] \quad (13)$$

$$= \int_0^t \int_0^{R_a} \frac{q\,r'}{2\sigma h(t-t')} \exp\left[-\frac{r^2+r'^2}{4a(t-t')}\right] B_0\left(\frac{rr'}{2a(t-t')}\right) dr'\,dt' \quad (14)$$

where:

B_0 is the Bessel function of the first order.

$$B_0\left(\frac{rr'}{2a(t-t')}\right) = \sum_{v=0}^{+\infty} \frac{1}{v!\,\Gamma(v+1)} \left(\frac{rr'}{4a(t-t')}\right)^{2v} \quad (15)$$

The temperature at any point on the inner face of the plate (depth h) at time t (t> t ') is given by:

$$T(r,t) = \frac{q_0 t}{c\rho h}\left(\exp(-u_1^2) - \left(1 + \frac{u_1^2 u_0^2}{u_2^2}\right)\exp(-u_2^2) - u_0^2\, Ei(-u_2^2)\right) \quad (16)$$

where:

$$u_0 = \frac{R_a}{2\sqrt{at}}\;;\; u_1 = \frac{r}{2\sqrt{at}}\quad and \quad u_2 = \frac{\sqrt{R_a^2 + r^2}}{2\sqrt{at}}$$

World Academy of Science, Engineering and Technology
International Journal of Electrical and Computer Engineering
Vol:7, No:11, 2013

with $\quad Ei\ (-u^2) = \int_{u^2}^{\infty} \frac{\exp(-x)}{x} dx$

Ra is the radius of the cathodic or anodic spot;
h is thickness of the plate.
for the case r = 0, we have:

$$T\ (0,\ t)\ =\ \frac{q_0\,t}{c\,\rho\,h}\,(1\,-\,i\,Ei\ (-u_0^{\,2}\,)) \qquad (17)$$

C. The Numerical Resolution

In the numerical solution of the two-dimensional geometry [9], the calculation can be done digitally and the resolution heat equation in each of the solid and liquid phases leads to the following system of (18):

$$\frac{\partial T}{\partial t} = a_s \nabla^2 T\ \ for\ \ T_0 < T < T_{fusion}\ \text{(solid phase)} \qquad (18)$$

$$\frac{\partial T}{\partial t} = a_\ell \nabla^2 T\ \ for\ \ T_{fusion} < T < T_{vaporisaon}\text{(liquid phase)}$$

a_s and a_ℓ are respectively the thermal diffusivities of the solid state and the 'liquid state of the metal, (m² / s).
$\nabla^2 T$ is the Laplacian of the temperature T which is given in cylindrical coordinates r, θ, z .

We used the method of finite differences. Various numerical methods for solving the system (18) can then be implemented, among which there are the explicit and implicit methods. According to the explicit scheme, we can discretize this system in the following form:

$$\frac{T_{i,j}^{n+1} - T_{i,j}^{n}}{h} = a_{ph} \nabla^2 T_{i,j}^{n} \qquad (19)$$

$a_{ph} = a_\ell$ for the liquid phase

$a_{ph} = a_s$ for the solid phase;

$T_{i,j}^{n} = T(i, dr, j, dz, n, h)\ \ 1 \leq i \leq I;\ 1 \leq j \leq J$

dr and dz are the spatial steps;
h is the time step;

$\nabla^2 T_{i,j}^{n}$ depends on: $T_{i,j}^{n};\ T_{i-1,j}^{n};\ T_{i+1,j}^{n};\ T_{i,j-1}^{n};\ T_{i,j+1}^{n}$.

By this method the explicit calculation is very fast but not enough accurate and its stability is conditional. Some theoretical considerations show that it is better to use the implicit type method which overcomes the problems of stability and provides more accurate results [9]. This principle involves taking the Laplacian of the temperature not at the time n, but at the time n +1.

$$T_{i,j}^{n+1} = T_{i,j}^{n} + h\ a_{ph}\ \nabla^2 T_{i,j}^{n+1} \qquad (20)$$

IV. EXPERIMENTAL RESULTS

At this stage, we measure the speed displacement of the according to the arc current for different values of magnetic blowing. This experiment is made for different materials such as copper and aluminum. When the arc passes, the speed sensor records its pulses at the latter's output. The average speed is calculated by the following formula:

$$V_{moy} = \frac{x}{t} \qquad (21)$$

x: distance between the first and the last photodiode.
t: time taken for the course (s).

A. The Copper Materials

To study the speed of the arc, it is necessary to measure the magnetic blowing. Indeed, the measurement of the magnetic field created by the blowing coils between the electrodes is achieved using a flowmeter connected to a coil having 40 circular turns. The induction of the magnetic field (B) is then given by the following relationship:

$$B = \frac{\phi}{40\ S} \qquad (22)$$

where:
ϕ is the measured flux.
S is the surface area of a turn.

The experimental results for copper electrodes are shown in Table I.

TABLE I
DIFFERENT MEASURED BLOWING VALUES FOR COPPER ELECTRODES

B (Tesla) / I (A)	B1	B2	B3	B4
I= 8.5 A	0.001	0.01	0.011	0.015
I= 17 A	0.006	0.012	0.015	0.024
I= 26 A	0.008	0.026	0.026	0.035
I= 35 A	0.02	0.05	0.04	0.059

The average speeds of movement of the arc (in m/s) depending on the magnetic blow and current are presented in Fig. 4.
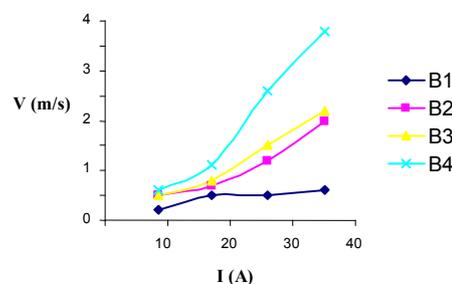

Fig. 4 Speeds of the arc movement for different values of blowing in the case of copper electrodes

World Academy of Science, Engineering and Technology
International Journal of Electrical and Computer Engineering
Vol:7, No:11, 2013

B. The Aluminum Materials

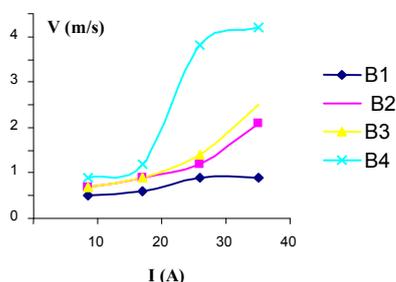The measurement results for an arc with aluminum electrodes are shown in Fig. 5.

Fig. 5 The speeds of the arc movement for different values of blowing in the case of the aluminum electrode

Since the magnetic induction is dependent on the current excitation, several researchers have shown that the average speed of movement of the arc can be expressed by the following equation [10]-[11]:

$$V = K \ I^{\alpha} B^{\beta} \qquad (23)$$

We have determined experimentally the coefficients α and β. The results are as follows:

$$\text{Copper: } V = 100 \ I \ B^{0.8} \qquad (24)$$

$$\text{Aluminum: } V = 100 \ I^{1.1} B^{1.2} \qquad (25)$$

The required objective is to verify through experiments the melting contacts model by translating the arc on a horn shaped electrodes. The calculation allows determining the size of the melted bath at any time according to the density of the heat flow provided by the arc. In order to validate the thermal model of the displacement arc by experience, we wrap electrodes by thin films of different thicknesses (Fig. 6). Note that the material of the film used to wrap the electrode is of the same nature than that of the electrode. Films are dismantled after the action of the arc to verify if the melting temperature attacks all its thickness Δ. The fusion model is validated once the calculation results Δ prove that the melting temperature reaches the inside face of the plate and it undergoes drilling.

Fig. 6 The photograph of a test electrode copper of 1mm thickness

On the surface of the electrode shown in Fig. 6, we see only the traces of the arc as the electrode is not pierced. The main results obtained with copper electrodes are given in Table II:

TABLE II
THE MEASURED SPEES CAUSING OR NOT THE PERFORATION OF COPPER

Copper		Observed speeds causing perforation or not
Δ=0.05 mm	I=8,5 A	for 0.2 m/s performed
		for 0.5 m/s performed
		for 0.6 m/s performed
Δ=0.5 mm	I=26 A	for 0.5 m/s performed
		for 1.2 m/s performed
		for 1.5 m/s performed
		for 2.6m/s not performed
Δ=1 mm	I=35 A	for 0.6 m/s performed
		for 2 m/s performed
		for 2.2 m/s not performed
		for 3.8 m/s not performed
Δ=2.5 mm	I=35 A	for 0.6 m/s performed
		for 2 m/s not performed
		for2.2 m/s not performed
		for 3.8 m/s not performed

The same experiment carried out with aluminum electrodes led to the results shown in Table III.

World Academy of Science, Engineering and Technology
International Journal of Electrical and Computer Engineering
Vol:7, No:11, 2013

TABLE III
THE MEASURED SPEEDS CAUSING OR NOT THE PERFORATION OF THE ALUMINUM

Aluminum		Observed speeds causing perforation or not		
Δ=0.01 mm	I=8,5 A	for	0.5 m/s	performed
		for	0.7 m/s	performed
		for	0.9 m/s	performed
Δ=0.02 mm	I=17 A	for	0.6 m/s	performed
		for	0.9 m/s	performed
		for	1.2 m/s	performed
Δ=0.05 mm	I=17 A	for	0.6 m/s	performed
		for	0.9 m/s	performed
		for	1.2 m/s	not performed
Δ =1 mm	I=17 A	for	0.6 m/s	performed
		for	0.9 m/s	not performed
		for	1.2 m/s	not performed
Δ =1.5 mm	I=26 A	for	0.4 m/s	performed
		for	0.6 m/s	not performed
		for	1.2 m/s	not performed
		for	1.4 m/s	not performed
		for	3.8 m/s	not performed

Aluminum is less erosion resistant than copper. The currents used are weaker. In Figs. 7 and 8 the areas of speed limits that can cause perforation of copper and aluminum are respectively represented.
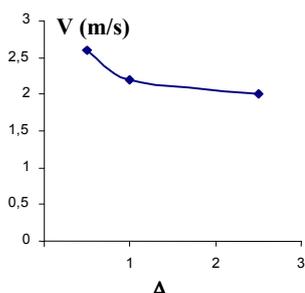

Fig. 7 The speed limits causing the perforation according to the thickness of the electrode for copper
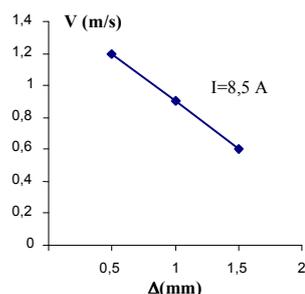

Fig. 8 The speed limits causing the perforation according to the thickness of the electrode for the aluminum

Note that speed is equivalent to the stagnation time of the arc.

V. EROSION CALCULATION

Given the complexity of the mechanism which causes the ejection of the metal surface of the electrode submitted to an electric arc (the metal vapor discharge as jets of plasma ejection of liquid droplets are ejected and sometimes solid metal), the manufacturers of the electrical switchgear failed to establish a method for calculating the erosion and are based solely on experiments to check this phenomenon. The study achieved using rapid cinematography showed that after a given time, a certain amount of liquid metal is formed on the surface of the electrode, and even ejected depending on the density of the heat flow provided by the electric arc [7]. This is very important because the amount of the ejected liquid metal is not necessarily constituted by the totality of the formed melt, but depends on the balance of forces on the surface of the electrode, thus it refers to what depends on the current density and the arc duration. Therefore, the total erosion is the amount of the vaporized metal is added to the ejected metal. Therefore there will be:

$$M = m_v + Kej.m_f \qquad (26)$$

where:
 M: the total weight of erosion;
 m_v: the mass lost by vaporization;
 m_f: the melted mass material;
 Kej: the ejection coefficient of the liquid metal with a value between 0 and 1.

The expression (26) shows that the erosion varies between a minimum value in the absence of the ejection phenomenon and a maximum value when the entire liquid bath formed is ejected. The aim is to develop a method for estimating the amount of ejected molten metal. This method can be summarized by determining the ejection coefficient (K_{ej}) which is based on a set of experimental results and those of erosion calculation according to the thermal model. In this study, our focus was on the example of a lithotripter used for the fragmentation of kidney stones. In this unit, we look for homogeneous materials that may eventually replace the composite material constituting the electrodes without causing excessive durability decrease. Because iron and molybdenum come in large quantities in the constitution of the electrode material of the lithotripter, it was considered necessary to choose them and copper as alternative materials. Indeed, the value of the total erosion of these materials is given by Wilson [12] who measured the loss volume for a total current of 12 kA and the duration of the arc existence of 8 ms for different Table IV materials:

TABLE IV
THE VOLUME EROSION FOR I=12 KA AND t= 8 ms

Material	Mo	Fe	Cu
Erosion(cm3/kA.s)	0.7	1	1.8

For determining Kej, it remains only to calculate volumes melted and sprayed for the same conditions of experiment by Wilson [12]. However, to calculate the size of the molten bath, it is necessary to know the parameters of the model, in particular the density of the flow of heat provided by the arc. It is expressed by [13]:

$$q = JUeq \qquad (27)$$

World Academy of Science, Engineering and Technology
International Journal of Electrical and Computer Engineering
Vol:7, No:11, 2013

Ueq: the equivalent voltage of the arc in the vicinity of the electrode is determined by experiments;

J: the current surface density.

To obtain an equivalent voltage equals to 10 V and a heat flow density $q=5.10^9$ W/m^2, we calculated volumes of bath melted and vaporized for these materials. The calculation results are presented in Table V [13]:

TABLE V
THE VOLUMES OF THE CALCULATED BATHS MELTING AND VAPORIZATION FOR I=12 KA, t=8ms

Material	Fe	Mo	Cu
Vaporized volume (cm^3/kA.s)	0.41	0.3	0.55
Melted volume (cm^3/kA.s)	2.3	1.4	3.1

The superposition of the calculated results (Table V) and the experimental results of erosion (Table IV), allows according to (25), to deduce the ejection coefficient for each material (Table VI).

TABLE VI
THE EXPERIMENTAL EJECTION COEFFICIENTS FOR I=12 KA AND t=8 MS

Material	Fe	Mo	Cu
K_{ej}	0.25	0.28	0.4

It is appropriate to use those results for calculating the total erosion of iron, molybdenum and copper in the operating conditions of the lithotripter. We will initially start with the calculation of volumes and sprayed molten metal in the three operating conditions of the lithotripter Indeed, as it is recognized in the literature that the density of heat flux in a gas is 1.5 times lower than that in a liquid [13], we will use a value of the order q of $7.5.10^9$ W/m² [14], [15]. We recall that in the case of the lithotripter the discharge duration is equal to 2μs. Fig. 9 shows the penetration of the melting front (zone II) and the vaporizing front (zone I) in the case of an iron electrode. This metal has a melting temperature of about 1530°C and a vaporizing temperature approximately equal to 2450 °C.
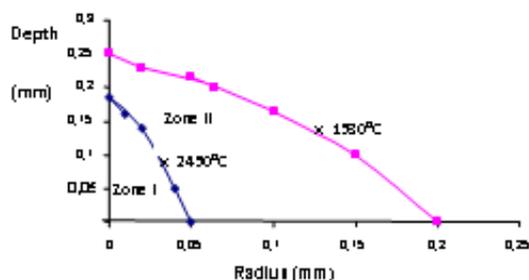

Fig. 9 The isotherms of temperature for an iron electrode
$q=7,5.10^9$ Wm^2

Calculations have also been made for molybdenum and copper, the calculation results are summarized in Table VII.

TABLE VII
THE VAPORIZED AND MELTED BATH VOLUMES CALCULATED FOR q= 7,5 109 W/m²

Material	Fe	Mo	Cu
Erosion by Vaporization (mm^3)	3 .10-3	1,1 .10-3	11,5.10-3
Possible maximal erosion of melted bath (mm^3)	32 .10-3	19. 10-3	108. 10-3

We can, therefore, say that the total erosion of each material is determined by the calculated volumes of the vaporized and the melted bathroom presented in Table VII and the discharge coefficient calculated for the conditions of Wilson. (I= 12kA and t= 8ms). [13] Table VIII presents the results of the total erosion calculated by (23) for the operating conditions of the lithotripter:

TABLE VIII
VOLUMES OF TOTAL CALCULATED EROSION FOR THE OPERATING CONDITIONS OF THE LITHOTRIPTER

Material	Fe	Mo	Cu
Kej	0,3	0,3	0,4
Total Erosion (mm^3)	12.6 .10-3	6.8 .10-3	54.7 .10-3

Table VI shows the conditions of Wilson experience (I=12 kA and t =8 ms), the ejection coefficient is about 0.25 for iron, 0.28 for molybdenum and 0.4 for copper. These conditions are similar to those of the operation of electrical equipment with the strong currents where the arc time existence does not exceed 10 ms and the current is a few tens of kA. These results can be used to estimate the erosion of the contacts of switch units. The proposed thermal erosion calculation model is based on the experimental results, and it includes the calculation of the material heating with an evaluation of the mass lost by vaporization as well as the mechanisms of ejection.

VI. CONCLUSION

The aim of the manufacturers of electrical breaker apparatuses is to improve the durability of the contacts which determines in many cases the life of the entire apparatus. To apprehend these problems, we started with a detailed analysis of the phenomena occurring at the electrodes and which showed that erosion during contacts opening is the primary factor which limits the durability of a contact. The analytical methods are limited to cases in which the geometry is one-dimensional and can show the behavior of different materials. The method used is Green's function which is widely used in solving thermal problems. This function expresses the function point source and can enable the transition to the source surface. The modeling must include the estimation of the lost mass due to the vaporization and the ejection of droplets. This phenomenon is important because the amount of the ejected metal is not necessarily constituted by the totality of the melt formed and depends on the balance of forces at the contact surface. We have shown that the decoupling of equations acting is complicated. To this end and in order to calculate the ejection coefficient, we proposed a method which consists in comparing the experimental results with the

World Academy of Science, Engineering and Technology
International Journal of Electrical and Computer Engineering
Vol:7, No:11, 2013

calculated ones. On the other hand, it would be appropriate to conduct an extensive research on some aspects of the issue of erosion by the arc that has not been fully covered by this work, namely the problem of the droplet-ejection and the mechanism of extraction of the liquid or solid metal. Concerning these two phenomena, it is recommended to develop experimental measurements of the force applied by the arc in a systematic study valid for both homogeneous materials and composite materials. Alternatively, it is note that currently we have a large database of erosion and that the presentation of these results could contribute to the resolution of certain contact erosion problems.

REFERENCES

[1] M. W. Baldwin, "Electric arc furnace impact on generator torque". Power Systems conf and expo, IEEE PES. 2004, vol 2, pp. 776-780.

[2] I L Babich, A L Cheredarchuk, A Veklich N, and V V.A. Zhovtyansky, "Spectroscopic investigations of the cathode region of the three burning copper arc. Discharges and electrical insulation in vacuum", Proceedings ISDEIV, XVIIth Int Symp, 1998, vol 1, pp. 215-218.H. Poor, *An Introduction to Signal Detection and Estimation.* New York: Springer-Verlag, 1985, ch. 4.

[3] G. Rego, l. m. n.b f. Santos, B. Shroder, V S Maques and J.L. Santos, "In situ temperature measurement of an optical fiber submitted to electric arc discharges. Photonics technology letters, ieee, 2004, vol 9, pp. 2111-2113.

[4] R L Doughty, T E Neal, G M Laverty, and H. Hoagland, "Electric arc hazard assessment and personnel protection" . Industry applications conf record IEEE, 2000, vol 4, pp. 2782-2789.

[5] C. Turner, H. Turner h, F. Frey, "The relation between wear of copper contacts and arc current". ERA Report, - Ref. 5119, 1996.

[6] A. misserand., "Conductivité thermique ", Editions Eyrolles, Paris, 1965, p 554.

[7] J.P. charberie, J. deveautour and P H Teste,,"A numerical method for thermal process in an electrode submitted to an arc in air and its experimental verification". Holm conf on elect contacts, Philadelphia, 1992, pp. 65-70.

[8] H.S. Carslaw,, J.C Jaeger, "Conduction of heat in solids". Second Edition, Clarendon press, oxford,, 1990, p 375.

[9] D. Euvrand., "Résolution numériques des e.d.p" , Edition Masson. 1998.

[10] L. Féchant, "Le contact électrique". Edition Hermes, Paris, 1996.

[11] H. Allagui, A. Ouni and M. Javoronkov, "Forecast of the durability of the contacts of a contactor with the turning arc". Medium east symp on simulation and modelling, Sharjah, UAE, 2002, pp. 132-136.

[12] W. R. Wilson, "High current arc erosion of electric contact material". Trans. AIE, Pow & and Syst, 1965, pp. 657-664.

[13] H. Allagui, M. Mekki. and M. Javoronkov, "Electrodes erosion in a liquid medium".   IEEE Int Symp On Indus Electronics, Aquila, Italia, 2002, pp. 1289-1294.

[14] J. Deveautour, "Contribution à l'étude des interactions arc-électrodes. Influence de la structure métallurgique sur les mécanismes d'érosion des appareils de coupure". PHD of Paris 6 University.1992.

[15] V. Maxime, "Etude des mécanismes de défaillance du contact électrique dans un micro-interrupteur en technologie MEMS. PHD of Grenoble Polytechnique Institute, 2010.